An Expanding Foam-Fabric Orthopedic Cast

*Samuel E. Root, Vanessa Sanchez, Jovanna A. Tracz, Daniel J. Preston,
Yoav S. Zvi, Kemble Wang, Conor J. Walsh, Shervanthi Homer-Vanniasinkam,
and George M. Whitesides**

Traditional orthopedic casting strategies used in the treatment of fractured limbs, such as fiberglass and plaster-based tapes, suffer from several drawbacks, including technically challenging molding for application, occurrence of skin complications, and the requirement of a potentially hazardous oscillatory saw for removal, which is frightening for pediatric patients. This work presents the design and evaluation of a foam-fabric cast (FFC) to overcome these drawbacks by integrating strategies from soft materials engineering and functional apparel design. A fabric sleeve is designed to enable the reactive injection molding of a polymer foam and provide a form-fitting orthopedic cast for the human forearm—with sufficient mechanical reinforcement to stabilize a fractured limb. Through testing with a replica limb and human subjects with a range of forearm volumes, the FFC application process is demonstrated and characterized. The thermal, pressural, chemical, and hygienic safety are comparable to or safer than existing clinical technologies. The FFC weighs only ≈150 g, is water resistant, and represents a robust alternative to traditional casts that can be i) manufactured at a large scale for a low cost; ii) applied to patients simply, rapidly (≈5 min), and reliably; and iii) removed easily with a pair of scissors.

S. E. Root, J. A. Tracz, D. J. Preston, S. Homer-Vanniasinkam,
G. M. Whitesides
Department of Chemistry and Chemical Biology
Harvard University
Cambridge, MA 02138, USA
E-mail: gmwoffice@gmwgroup.harvard.edu
V. Sanchez, C. J. Walsh
John A. Paulson School of Engineering and Applied Sciences
Harvard University
Cambridge, MA 02138, USA
Y. S. Zvi
Department of Orthopaedic Surgery
Montefiore Medical Center
Bronx, NY 10467, USA
K. Wang
Royal Children's Hospital
50 Flemington Rd, Parkville, VIC 30152, Australia
S. Homer-Vanniasinkam
Department of Mechanical Engineering
University College London
London WC1E 7JE, UK

The ORCID identification number(s) for the author(s) of this article can be found under https://doi.org/10.1002/admt.202101563.

1. Introduction

Approximately 8 million orthopedic fractures are reported in the United States annually.[1] The most common form of medical treatment for pediatric patients with a long bone fracture, and some adult patients with nondisplaced fractures, is to immobilize and protect the limb during the healing process, typically using a cast molded from fiberglass or plaster. This approach requires the focused attention of a clinician during the processes of application and removal (≈20 min each session).[2] Casting also carries a risk of skin complications due to thermal injury or sharp cast edges, difficulty in monitoring swelling of soft tissue, and the need to keep the cast clean and dry in a typically noncompliant adolescent patient.[3] Moreover, the cast removal process is particularly problematic for pediatric populations, who are often distressed by (and in some cases injured by) the oscillatory saw used for cast removal.[4] The time and challenge of application, potential for iatrogenic injury and skin complications, as well as the costs associated with the application and removal of these casts offer significant potential for improvement using modern textile and soft robotic approaches.[5]

The earliest examples of modern orthopedic casts were developed in the mid-19th century using cotton bandages containing plaster of Paris.[2] Although plaster of Paris still finds use in modern orthopedic practice for splinting purposes, knit fiberglass bandages impregnated with polyurethane were introduced in the 1970s as an alternative technology. Such fiberglass casts are more permeable to X-rays, weigh less, solidify faster, and are more durable than plaster casts.[2] They are, however more expensive and less malleable (not as easily molded during application) than plaster casts.[2] Fiberglass casts are often used as definitive treatment for pediatric fractures, requiring prolonged periods of immobilization. Their circumferential application makes skin monitoring difficult and may require cast valving using an oscillatory saw to allow for swelling. The process of cast valving, while reducing the risk of compartment syndrome (tissue damage caused by the blockage of circulation due to excessive pressure), also introduces the risk for the loss of fracture reduction.[6] Plaster casts are reserved for

**ADVANCED
SCIENCE NEWS**
www.advancedsciencenews.com

**ADVANCED
MATERIALS
TECHNOLOGIES**
www.advmattechnol.de

splinting fractures that require more significant reduction (i.e., manual alignment of the displaced bones) or more intricate molding,[2] and are more accommodative in patients with significant swelling. A problem inherent to both of these materials is the requirement of an oscillating saw for removal, which can scare pediatric patients and, in up to 4.3% of cases (during the training of orthopedic residents), cause injuries and ensuing medicolegal liabilities.[7–9]

A variety of strategies have been introduced to circumvent the problems associated with fiberglass- and plaster-based tapes. One clinically available strategy that circumvents the requirement of an oscillatory saw for cast removal is the Soft-Cast, a soft fiberglass casting tape that can be unrolled or cut with bandage scissors to remove.[10] Due to the low stiffness of this cast, however, it is only recommended for pediatric patients who weigh less than 20 kg, and clinicians remain concerned about its mechanical strength in the reinforcement of potentially unstable fractures.[10] "Off-the-shelf" splints represent an option for sprains and hairline fractures, but are not custom molded to the patient, do not provide sufficient mechanical stability compared to plaster or fiberglass, and introduce issues with patient compliance.[11] Thermoformable braces have also found clinical use, and can be molded by a clinician in a manner that is easier than fiberglass or plaster;[12] such braces are more costly than fiberglass or plaster and require an external heating chamber to prepare the material prior to brace application, which may not be available in a field setting. Customized casts based on 3D scanning and additive manufacturing are also being actively explored,[13] and offer great potential given the rapid advancement and adoption of 3D printing technology.[13–15] Yet this customized approach has the drawbacks of high cost, long production time, and the requirement of equipment not found in all medical centers.[13–15] Another recently developed approach uses a web of flexible tubing into which a liquid can be injected and photocured to solidify. This is a practical technology for fractures and sprains to increase patient comfort and circumvent the requirement of a cast saw for removal, however, it requires a UV light source for activation.[16]

In this work, we designed and evaluated a new type of cast based on the expansion and solidification of a rigid polymer foam within a custom garment sleeve: the foam-fabric cast (FFC; **Figure 1**). The FFC has a fabric exterior, with an interior thermoplastic pouch that functions to distribute the foaming liquid, guide its uniform expansion around the limb, and vent excess gas to prevent the build-up of pressure. A prestrained fabric inner lining at the cast–skin interface stretches during the expansion process to conform to the contours of the wrist without the formation of wrinkles (i.e., areas of localized pressure, where dermal irritation typically arises). The FFC design also incorporates an overlapping region of foam held together by a fabric band that can be cut with scissors, precluding the use of an oscillatory cast saw for removal. The use of an expanding polymer foam eliminates the requirement of custom-molding and provides a safe, reliable process for application and removal without the sacrifice of mechanical support, patient comfort, or manufacturability.

Figure 1. The expanding foam-fabric cast (FFC). a) A schematic diagram describing the application process. b) A photograph showing the expanded FFC on a wrist. Scanning electron microscope (SEM) images showing c) the knit laminate, d) the spacer knit fabric, and e) the rigid foam. SEM images are false colored to reflect the colors of the respective materials. f) A transverse section of the cast obtained from X-ray computed tomography.

2. Design

2.1. Selection of Foam

We used a rigid polyurethane foam as the primary structural support component for the FFC based on two considerations. First, when the foaming reaction is initiated, the liquid undergoes a simultaneous expansion and solidification process, such that it molds to the shape of the object that constrains its expansion (i.e., a foam-in-place process);[17] the gas produced during this process is CO_2, and thus presents no potential harm to the patient or medical professional. Second, the cellular structure allows the foam to be lightweight while retaining mechanical strength.[18,19] Similar considerations have motivated the invention of a splinting method based on the spraying of a foam (containing isocyanate precursors) directly onto an injured appendage during an emergency or field situation;[20] spraying isocyanate derivatives directly onto injured limbs, without a barrier, could result in contact dermatitis.[21]

For our demonstrations, we used a commercially available, two-component methylene diphenyl diisocyanate-based polyurethane (PU) closed-cell foam with the following characteristics:

i) the reacting liquid expands to its full volume within 4 min, can be handled after 20 min, and is fully cured in 2 h; ii) the foam has an expansion factor of ≈18x, ensuring a conformal fit to the limb and a low mass density (≈0.048 g cm^{-3}); and iii) the foam costs only ≈$0.50 USD per cast. Moreover, such a formulation can be easily modified to increase or decrease the density of the foam[22] or the speed of the foaming reaction.[17] Foams of increased density were also evaluated, but the low density foam (≈0.048 g cm^{-3}) was selected after experimentally determining that casts made from this foam exhibited sufficient mechanical strength and required less material, reducing both cost of materials and the weight of the cast.[18,19] Moreover, we observed that the use of a foam with a higher expansion factor resulted in a more reliable foam-in-place process, where the homogenously expanding foam uniformly distributes throughout the cast, and thus forms a more conformal fit to the wrist.

2.2. Selection of Forearm as Model Limb

Our prototype was designed for the forearm or wrist, as fractures of the distal radius are particularly prevalent, accounting for ≈25% of fractures in the pediatric population and 18% of all fractures in the elderly population, with data over the past 40 years indicating an upward trend in the incidence of these injuries.[23] Additionally, the high direct costs involved in treating this injury indicate an opportunity for our device to reduce a cost burden: the annual cost of treating distal radius fractures in the United States is upward of $2 billion USD for pediatric populations alone,[24] and the annual cost burden of this fracture on Medicare (i.e., on the geriatric population within the United States) has been estimated to be up to $535 million dollars, and is expected to continue increasing.[25]

2.3. Design and Fabrication of Sleeve

Our cast consists of an exterior fabric sleeve (Figures 1 and 2) laminated to an interior thermoplastic polyurethane pouch that guides and constrains the foam's expansion. Although the thermoplastic films and closed-cell polyurethane foam have a low permeability to gas, ventilation holes passing through the laminated thermoplastic pouch allow for convective breathability of the cast, promoting patient comfort. In this design, there are four ventilation holes, but more could be added to increase breathability. **Figure 2**a shows the sheets of all fabric and thermoplastic materials used in the fabrication process. Figure 2b shows the pattern used to laser cut the respective films of materials.

The width of the stretchable inner knit spacer fabric (90% Polyester/10% Spandex) is smaller than the width of the outer knit polyester-thermoplastic polyurethane laminate fabric (Figure 2a) and is prestrained during the sewing process to mitigate the formation of wrinkles upon expansion. It is also shaped in such a way that its diameter as a function of length loosely matches that of the human forearm. In existing casts, wrinkling—caused by imperfect molding or uneven overlap in casting tape or padding—leads to an uneven distribution of contact pressure between the cast and the skin, with dermal

abrasion, irritation, or pressure sores.[3] The prestraining of the inner lining allows the garment to stretch into conformal contact with the skin as the foam expands. This strategy, in combination with the PU foam expansion properties, permits garments of two sizes (small and large) to support a range of patients with differently sized forearms (with forearm volumes of ≈500–900 mL corresponding to a small cast size and ≈900–1300 mL and corresponding to large; see subsection *Human Subject Testing*). In accordance with existing guidelines for short-arm casts, the fabric garment was designed to extend from the distal palmar crease to the proximal third of the forearm.[26] Importantly, all steps in the fabrication process are translatable to standard manufacturing processes from the garment industry.

2.3.1. Laminated Thermoplastic Elastomer Pouch

Figure 2c demonstrates the process used to heat press the pouch from films of thermoplastic elastomer (Stretchlon 200). Patterned films of parchment paper are used as a sacrificial layer to selectively bond the films (i.e., the films are only bonded in the regions where there is no parchment paper layer in between). The green film is bonded to the black laminated knit at each ventilation hole and along the perimeter.

Also using parchment paper, a four-way fluidic junction of channels is created within the thermoplastic pouch to uniformly distribute the injected foam to all four corners of the pouch so that the foam is uniformly distributed, and the expanded cast has a uniform thickness of foam. The optimal geometry of these channels was determined empirically. The channels were tapered (changing the width from 1.5 cm at the junction to 0.5 cm at outlet, over a length of 6 cm) and the corners were rounded to ensure that an approximately equal volume of foam would flow through each branch—and eliminate the possibility that all the liquid foam would flow out of one channel prior to reaching the ends of the others, as was observed with previous iterations. Heat pressing was performed at a temperature of 150 °C for a duration of 50 s, using an applied pressure of ≈10 kPa. The top and bottom of the pouch were not sealed until the final step of the process so that the parchment paper could be removed.

After sealing the pouch, a tube is inserted into the fluidic channel and held in place with a small piece of rubber sealant putty and electrical tape. The pouch is subsequently inflated with air and small holes are punctured throughout with a 16-gauge butterfly needle in the plastic film facing outward from the forearm. These holes allow excess gas (CO_2) produced by the foaming reaction to escape, preventing the formation of larger gas bubbles which otherwise would cause a build-up of pressure and inhibit the uniform distribution of the foam. The viscous foaming liquid does not leak through these small holes at the pressures produced by the expansion process. During human subject testing, we found that in some cases these pinholes alone were insufficient to prevent the build-up of excess pressure and modified the design to include a vent tube with a diameter of 0.5 cm for excess foam to escape, in addition to gas.

**ADVANCED
SCIENCE NEWS**

www.advancedsciencenews.com

**ADVANCED
MATERIALS
TECHNOLOGIES**

www.advmattechnol.de

Figure 2. Fabrication process. a) Photograph of sheets of materials used in fabrication of the FFC. b) Schematic diagram of the pattern used to laser cut these materials. c) Photographs of the cast at various stages of the fabrication process. Heat pressing, with patterns of parchment paper as sacrificial layers, is used to fabricate the thermoplastic pouch and fluidic channels for the foam. The red fabric pieces are sewn to the black fabric containing the green pouch (seams 1 and 2). The red fabric is then inverted through the thumbhole and seams 3 and 4 are sewn. Finally, the garment is inverted again, and the top and bottom seams (5 and 6) complete the fabrication process. A more detailed figure describing the fabrication process can be found in Figure S1 in the Supporting Information.

2.3.2. Sewing of Sleeve

Figure 2d shows the sewing process used to make the exterior fabric sleeve. A band of spacer fabric (1 in. wide) is first sewn onto the edge of the laminated pouch (seam 1). In the final sleeve form, this fabric band overlaps the cast on the ulnar side of the patient's wrist to allow for removal with scissors rather than an oscillatory saw. Moreover, overlap of the two sides of the plastic pouch ensures circumferential cast coverage: protection of the fractured limb is still present beneath this band. The inner spacer fabric is next sewn onto the laminated pouch along the circumference of the thumbhole (seam 2), through which the spacer knit is subsequently inverted. At this step, the tube connecting to the heat-sealed channels is punctured through a hole in the black knit laminate so that it is accessible from the exterior of the garment. Seams 3 and 4 are sewn in the inverted state, and then the cast is everted, before sewing the final top and bottom seams.

3. Results and Discussion

3.1. Application of Cast

To apply the cast, the liquid foam precursors are loaded into a 100 mL syringe fitted with a Luer lock valve. The syringe is shaken vigorously for ≈45 s; sufficient mixing is indicated by a uniform color of the mixed components. The mixed liquid, with a dynamic viscosity of 0.2 Pa s, is then injected over the course of ≈30 s through the valve that is secured to the cast by a Luer lock (**Figure 3**a–c). The foam travels through the channels into the interior of the TPU pouch and expands, conforming to the shape of the patient's wrist over the course of ≈3 min. Figure 3d shows X-ray photographs of this process. In our experiments, we have also found that there is an ≈1 min period of time where the liquid foam can be pushed around by squeezing the cast and a subsequent ≈2 min period during the expansion process where a gentle pressure to the cast's exterior can be used to
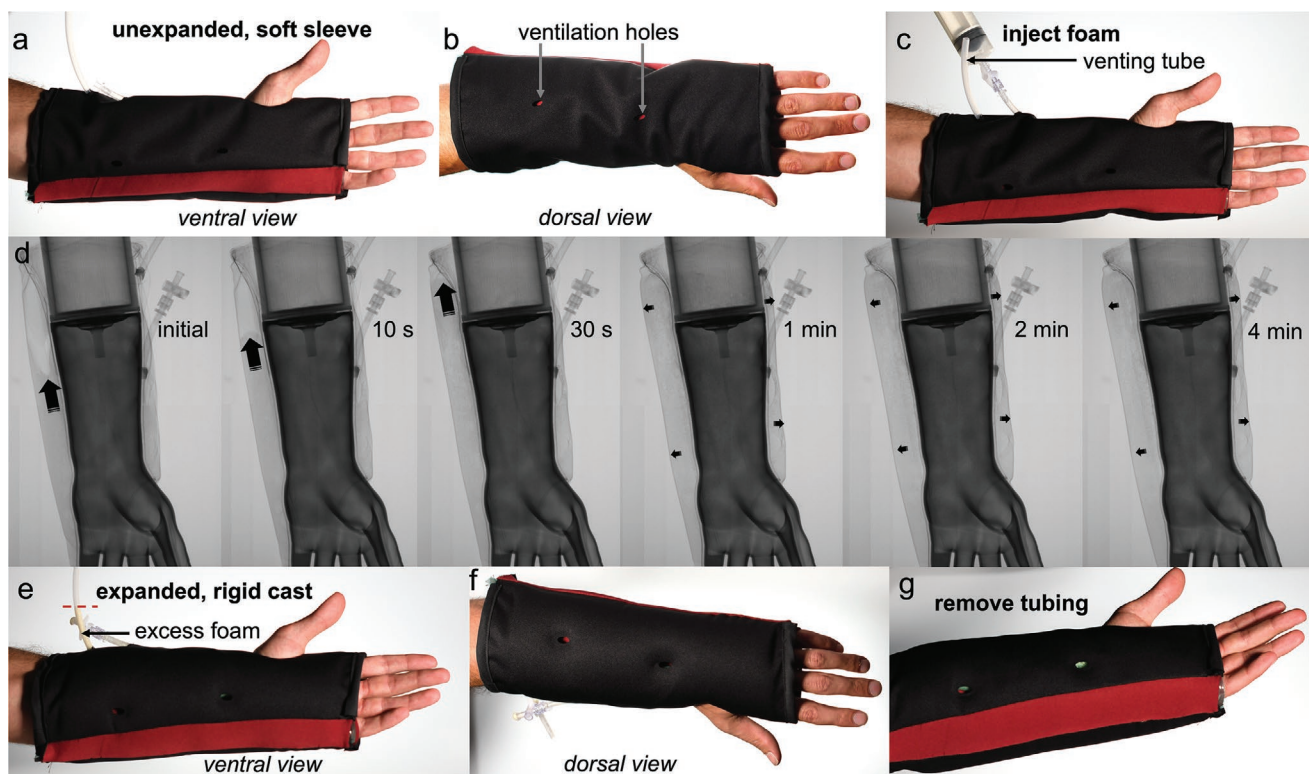
Figure 3. Application process. Photographs showing the a) ventral and b) dorsal view of the unexpanded, soft sleeve. c) A photograph showing the injection process using a syringe containing a valve with a Luer lock. d) X-ray absorption photographs showing the foaming liquid expanding and solidifying within the cast worn on a replica forearm. Photographs showing the e) ventral and f) dorsal aspects of the expanded, rigid cast. g) Photograph showing the cast following removal of the tubes used for injection and venting (they can be simply pulled out after the foam has stopped expanding).

mold the foam, which is unnecessary for effective application but can be performed if the clinician desires to make adjustments to the shape or reduce a displaced fracture. This window of time can be tailored for the specific needs of physicians by tuning the chemistry of the formulation based upon measurements of the time-dependent rheology during the foaming process. Figure 3e–g shows photographs of the cast following expansion and solidification. The cast is set ≈5 min after the foam is injected; and is fully cured in 2 h. In comparison, fiberglass casts can bear pressure ≈30 min post-application, while plaster can take up to 2 days to fully cure.[27,28]

3.2. Removal of Cast

A study of patients in the United States with fractures of the distal radius who subsequently had a cast removed by orthopedic residents revealed that up to 4.3% of these patients sustained cast-saw-related injuries.[7] Complications of cast saw use are typically i) abrasions or lacerations occurring when the blade comes into contact with the skin or ii) burns caused by the heat from friction between the saw blade and the cast material.[7–9] Historical data indicate expenses and indemnities paid for cast burn cases alone (excluding lacerations) ranged from $2995 to $25 000 per claim in the United Sates.[7] The FFC circumvents this issue with the fabric band overlap, which allows the cast to be removed with a pair of bandage scissors

(**Figure 4**). Underneath this fabric band exists an overlapping region of polyurethane foam, allowing for easy removal without the compromise of mechanical strength.

3.3. X-Ray Characterization with Replica Wrist

Testing and iterative development of the cast prototype was performed on a replica wrist, allowing for characterization using X-ray absorption photography (**Figure 5**a) and computed tomography (CT) analysis of the cast structure. CT scans provided i) proof that the prestrained inner spacer knit fabric prevented the formation of cast wrinkles in contact with the skin (Figure 5b), ii) confirmation of the uniform expansion of the foam (i.e., the absence of macroscopic bubbles of air), and iii) visualization of the foam expansion process within the cast (Figure 3d). These experiments also demonstrate the radiolucency of the FFC, an important attribute that would allow physicians to reduce displaced fractures (i.e., align the bones) during the casting process, and monitor the progression of bone healing without cast removal.[29,30]

3.4. Experiments with Human Subjects

To evaluate the safety and reliability of the cast application process, experiments with human subjects were performed using

**ADVANCED
SCIENCE NEWS**
www.advancedsciencenews.com

**ADVANCED
MATERIALS
TECHNOLOGIES**
www.advmattechnol.de

Figure 4. Photographs of the cast removal process using a pair of bandage scissors.

a total of seven adult subjects. Only two cast sizes (small and large) were required to span the range of volumes of the subject's wrists: ≈500–1300 mL, as approximately measured by displacement of water. Both cast sizes were kept the same length, but the circumference of the final cylindrical structure was reduced by 2 cm for the small cast by offsetting the width of the outer knit laminate and pouch. In initial experiments, 60 mL of foaming liquid was injected into small casts, and 65 mL was injected into large casts (without a ventilation tube). For casts with a vent tube (i.e., the final prototype), 70 mL was employed to ensure an excess volume of foam. During these experiments with excess foam, the foam traveled about an inch into the vent tube, but in no case did the foaming liquid start leaking out of the vent tube. For all experiments, the temperature and pressure were measured as a function of time during the cast application process using a thermocouple and a capacitive pressure sensor worn on the wrist.

3.4.1. Qualitative Assessment of Application Process

The subjects were asked questions to gauge the level of comfort during the casting process including the options of describing the experience as either uncomfortable, neutral, or comfortable. All subjects reported both the thermal and pressural experience of the cast application process as either neutral or comfortable

throughout the application process, with the thermal experience comparable to that of placing the arm in warm water. Subjects reported that the foam expansion felt uniform and that the pressure was evenly distributed with no localized spots of higher pressure. No subjects reported feeling that the pressure exerted by the cast was affecting the blood flow to their arm or that it felt uncomfortably hot on the skin. These qualitative reports agreed with our quantitative measurements, except in cases where drift of the capacitive pressure sensor reading was apparent (due to movements and stray capacitances of the subject[31]).

3.4.2. Thermal Safety

Given the exothermic nature of the foaming reaction,[21] the heat released during FFC application must be dissipated effectively to mitigate risk of thermal injury. Dermal temperature was monitored throughout the application process using a thermocouple inserted through the thumbhole of the cast and placed in contact with the skin (i.e., underneath the capacitive pressure sensing sleeve when present). **Figure 6**c shows the time series of the temperature measured in three different subjects. For subjects wearing a capacitive pressure sensor sleeve (an extra layer of thermal insulation and chemical barrier to ensure safety during initial experiments), the temperature peaked in the range of 35–42 °C ≈3 min after foam injection. For subjects with skin in direct contact with the cast, the temperature was slightly higher, peaking at 42–45 °C.

These temperatures are comparable to those experienced during both fiberglass and plaster cast application: fiberglass casts produce internal temperatures up to 45 °C and exhibit almost no risk of thermal injury during cast application, while plaster casts can produce internal temperatures >49 °C and exhibit only modest risks for thermal injury.[15] Thermal injury in the form of first-degree burns begins to occur when skin temperature exceeds 50 °C for at least 10 min,[15] which did not occur in our experiments. Moreover, the temperatures that we recorded were all below the threshold temperatures at which humans may begin to experience pain (47 °C) after prolonged exposure.[8] Additionally, the FFC application process precludes the use of dipping water: fiberglass and plaster cast application temperatures vary significantly and may reach dangerously high internal temperatures if the temperature of the dipping water and the amount of water squeezed out of the casting tape are not monitored.[17] From these experiments, and our observations throughout the design of the prototype, we found that the FFC has substantially equivalent thermal safety relative to the existing clinical technologies.

3.4.3. Pressural Safety

The pressure applied by an orthopedic cast should be minimized (under 30 mmHg) to prevent the constriction of blood flow.[32] Other thermoplastic casts have been shown to exert mean pressures of 31 ± 3 mmHg without occluding the microcirculation of the skin.[33]
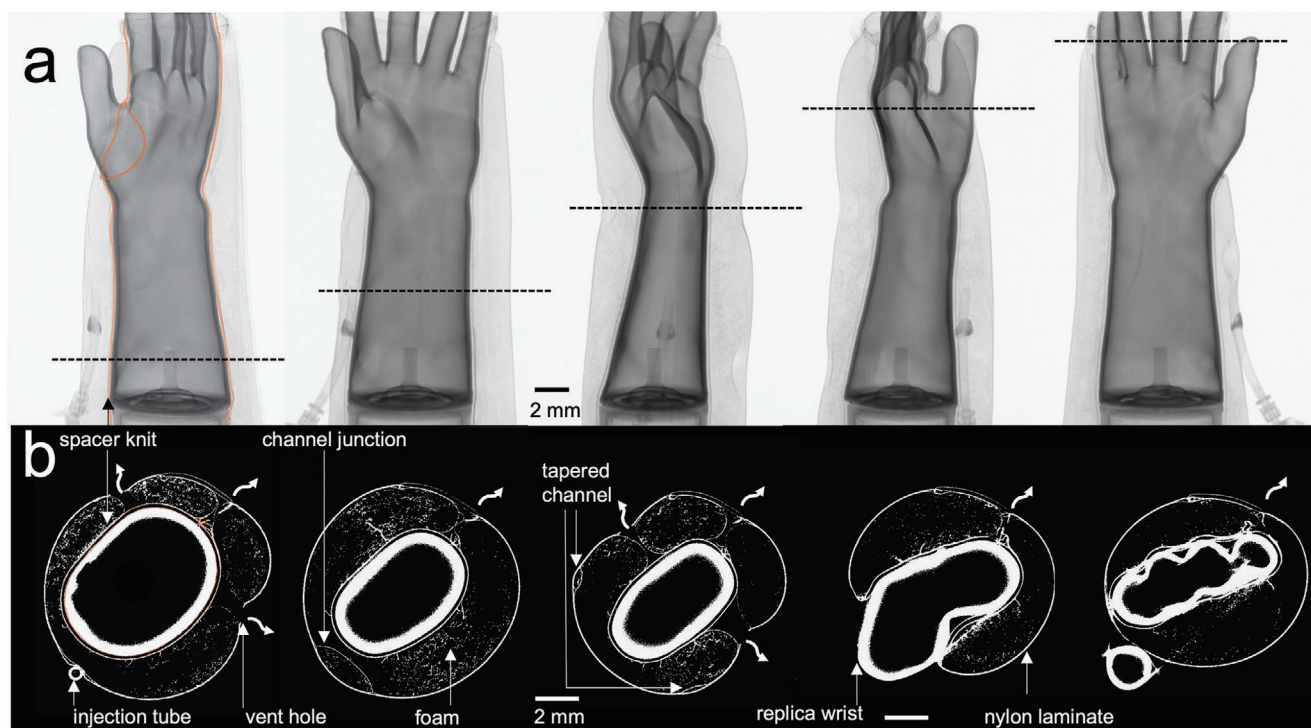
ADVANCED
SCIENCE NEWS
www.advancedsciencenews.com

ADVANCED
MATERIALS
TECHNOLOGIES
www.advmattechnol.de

Figure 5. X-ray computed tomography (CT) of the expanded cast on a replica forearm. a) Five X-ray absorption photographs showing positional rotations used to produce the 3D reconstruction. b) Transverse sections (post-CT reconstruction) of the cast showing that the inner spacer fabric stretches into conformal contact with the replica arm, without wrinkling.

In our experiments, the pressure was measured as a function of time using a capacitive sensing sleeve worn on the wrist of the subject underneath the cast, containing two co-facially arranged electrodes of conductive silver fabric heat-bonded to the opposite sides of the red spacer knit (Figure 1c), which served as the compressible dielectric layer for the capacitive sensing mechanism.[34,35] The electrical leads were soldered to the conductive silver fabric and the capacitance was read with an LCR meter at a frequency 10 kHz. The pressure sensor was calibrated immediately prior to each experiment using a medical grade pressure cuff (a sphygmomanometer) placed over the cast and over the sensor (Figure 6a). The pressure was manually increased in increments of 10 mmHg and held for 10 s while the capacitance was recorded to construct a linear calibration curve (Figure 6b).

We frequently observed drift in the measurement of capacitance arising from movements in the position of the wrist and stray capacitances from the human body.[31] This drift was corrected to the best of our ability by zeroing the baseline of the sensor during the initial foam injection and using only the slope of the calibration curve. An additional complication in the interpretation of these sensor readings is that the linear relationship between capacitance and pressure is also dependent upon temperature (Figure S2, Supporting Information), which increases during the first 10 min of the application process.

As an additional measure of pressure, we performed the following psychophysical experiment: we placed a blood pressure cuff on the subject's right wrist (i.e., the one without the cast) and gradually increased the pressure at a rate of 2.5 mmHg s^{-1} (without showing the subject the pressure reading) until the

subject reported that the pressure exerted by the cuff on their right hand matched the pressure exerted by the orthopedic cast on their left hand. We found that values of final pressure determined by both methods generally produced consistent results, except in cases where sensor drift was apparent. The measurements with the capacitive pressure sensor were difficult to interpret for the cases in which the pressure remained below 20 mmHg but gave a clear reading when the pressure exceeded 20 mmHg. Excess build-up of pressure was also readily visible in the shape of the expanded cast (inset of Figure 6f). Overall, the pressure reported by comparison to the pressure cuff appears to be more reliable than the sensor reading due to difficulties in disentangling sensor drift.

For the four adult male forearms used in the trial (with volumes ranging from 800 to 1300 mL), the same size cast was used, and the same volume of foam was injected (65 mL). A clear correlation between volume of the subject's arm and pressure reported was not observed (Figure 6d). We ascribe this lack of correlation to variability of the expansion factor of the foam, probably due to a lack of precision in the stoichiometry of the two components and variability in the manual mixing procedure. In the subject with the largest forearm (subject 3, 1300 mL), the pressure was built up to ≈40 mmHg and the cast assumed a more bulbous shape. These observations indicated that an additional mechanism was required release excess foam (in addition to gas through the pin holes in the pouch) to allow the same sized cast to span a wider range of arm volumes, without exerting too much pressure.

To address this issue, we incorporated a ventilation tube with an inner diameter of 0.5 cm to the proximal end of the cast
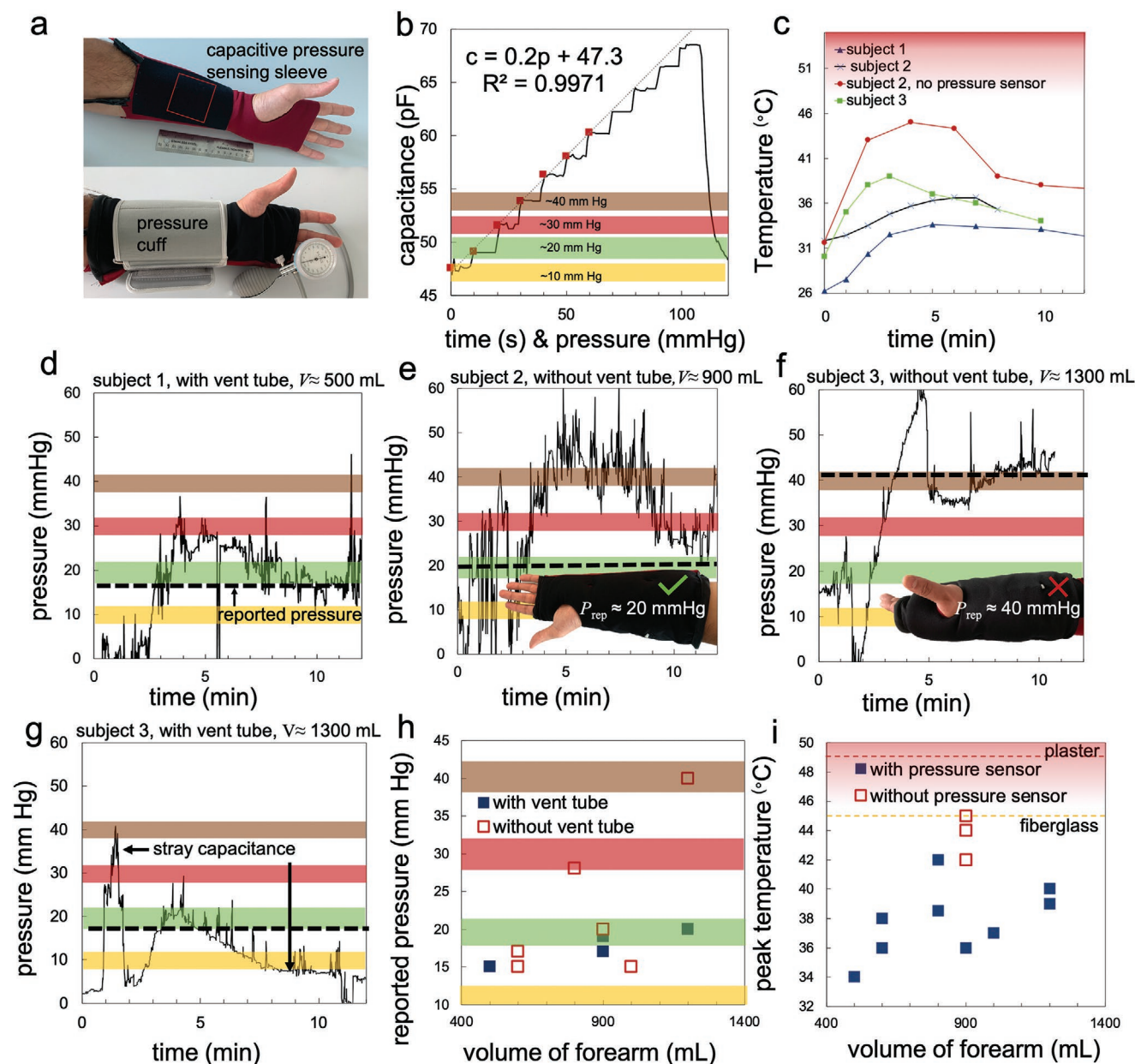
Figure 6. Experiments with human subjects demonstrating the safety and reliability of the FFC application process. Bolded, black dashed line represents the pressure reported by the subject in comparison to the sphygmomanometer. a) Photographs of the capacitive pressure sensing sleeve and the cast during the calibration process. The active area of the pressure sensor is indicated by the red outline. b) Plot showing the linear relationship between sensor capacitance and pressure, determined during calibration. c) Plots of the temperature (measured using a thermocouple in contact with the skin) as a function of time after foam injection into casts on subjects 1–3. Plots showing the time series of pressure measured by the capacitive sensor for d) subject 1, with a vent tube; e) subject 2, without a vent tube; and f) subject 3 without a vent tube, where the pressure builds up above 30 mmHg (see inset photograph of bulbous cast), and g) with a vent tube, where it does not. Sensor drift arises due to stray movements of the subjects' arms and stray capacitances from their bodies. h) Plot of the pressure reported by the subject versus the volume of their forearm. Two of five casts without vent tubes built up excess pressure >30 mmHg. Casts with vent tubes all exhibited pressures ≈20 mmHg, even when excess foam was added. i) Plot of the maximum temperature recorded versus the volume of the forearm.

(Figures 1–3). When this modified cast was applied to subject 3, we observed that both excess gas and foam were permitted to exit the cast through the tube, preventing the excessive build-up of pressure and the associated bulbous cast shape (Figure 6f). We believe that uniform foam coverage, an optimized fit to the patient's wrist, and overall reliability of the application pro-

cess in a clinical setting would be best achieved by using an excess amount of foam with this venting tube. To demonstrate this concept, we performed two additional tests on subject 2, in which the volume of foam injected was increased to 70 mL. We observed that the cast produced the same amount of pressure (≈20 mmHg) and more foam escaped through the vent
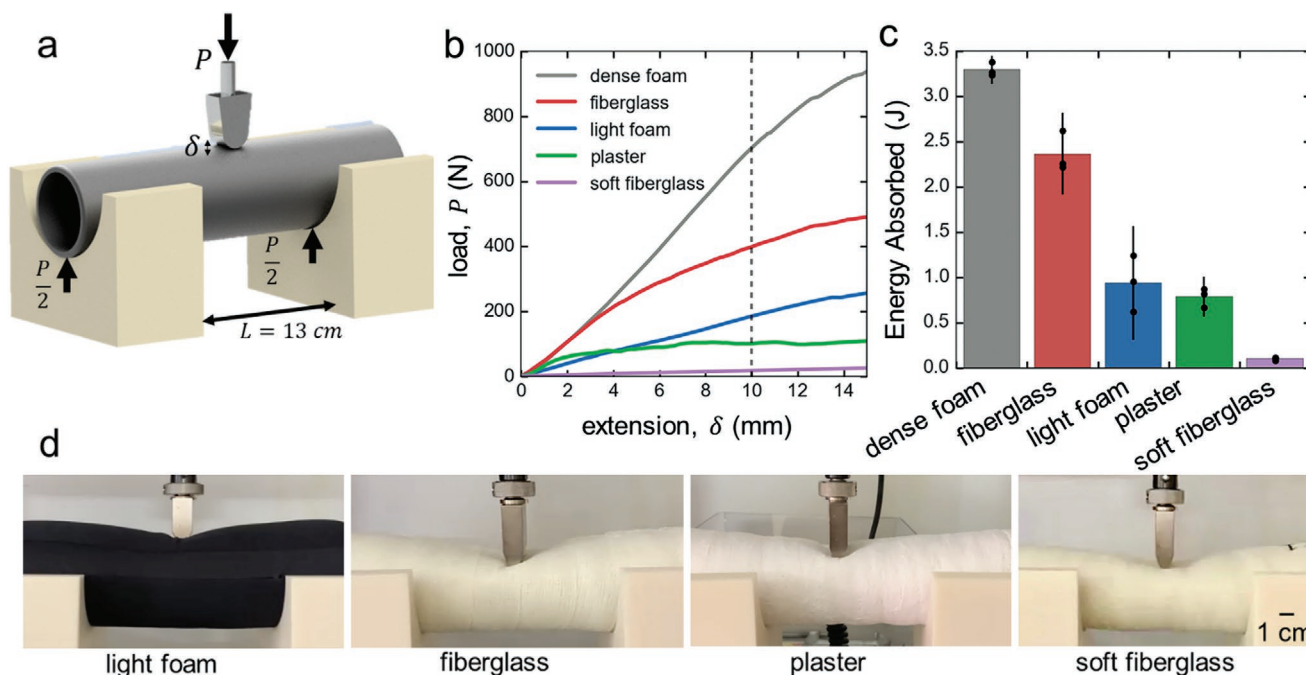
ADVANCED
SCIENCE NEWS
www.advancedsciencenews.com

ADVANCED
MATERIALS
TECHNOLOGIES
www.advmattechnol.de

Figure 7. Three-point flexural testing. a) A schematic diagram showing the experimental set up for the three-point flexural testing of the hollow cylindrical samples. b) A plot showing the load versus extension curves for the various casting materials investigated. c) A bar chart showing the mean mechanical energy absorbed by each hollow cylinder upon indentation to 10 mm. The data points show the scatter from three independent experiments for each material, and the error bars represent 95% confidence intervals of the mean from these experiments. d) Photographs of hollow cylindrical samples under flexural loading. FFC's made from "light foam" (density 0.048 g cm^{-3}) and "dense foam" (density 0.08 g cm^{-3}) were compared to "fiberglass" (3M Scotchcast Rigid Casting Tape), "plaster" (BSN Medical GYPSONA Plaster of Paris), and "soft fiberglass" (3M SoftCast) casting materials.

tube (although still not reaching the end of the tube before solidifying). Further evidence that casts formed this way did not produce excessive pressure was obtained by performing a three-day field test, in which the cast was worn during daily activities including showering, swimming, typing, eating with utensils, and writing with a pencil. During this qualitative field test, no effects of inhibited circulation (e.g., skin discoloration, decreased sensation) were noted. The full set of recorded pressure data is presented in Figure S3 in the Supporting Information.

3.5. Three-Point Flexural Testing of Mechanical Stability

The function of an orthopedic cast is to mechanically stabilize a fractured bone during healing. To provide a preliminary evaluation of the efficacy of the FFC under clinically relevant loading conditions,[28,36] we conducted symmetric three-point flexural tests of hollow cylindrical samples of the FFC, the fiberglass cast (3M Scotchcast Rigid Casting Tape), the plaster cast (BSN Medical GYPSONA Plaster of Paris), and the soft fiberglass cast (3M SoftCast). All samples had a length of 30 cm, an inner diameter of 7 cm, and a thickness of ≈ 1 cm) (**Figure 7**). All casts were applied to a pipe and removed by sliding the cast off the pipe after allowing for it to cure. Fiberglass and plaster casts were applied to the pipe according to manufacturer guidelines, including use of the recommended stockinette and cotton padding. The initial slope of the load versus extension curve gives the overall stiffness (N m^{-1}) of the structure with respect to the

imposed three-point bending mode. Figure 7b shows that the stiffness of the foam cast can be modified by altering the density of the foam: a cast made from a denser foam (0.08 g cm^{-3}) had a stiffness comparable to that of fiberglass, and a cast made from a light foam (0.048 g cm^{-3}) had a stiffness comparable to a plaster cast. Both foam casts tested were stiffer and stronger than the SoftCast. The total work at a displacement of 1 cm, denoted as "strength" in **Table 1**, was calculated to provide a figure of merit to compare the relative strengths of the casting materials (Figure 7c). The strength to weight ratio was also computed by dividing by the measured strength by the average mass of each cast (Table 1). We conclude from these experiments and analyses that the mechanical properties of the foam cast can be tuned to either improve upon or provide substantially equivalent mechanical reinforcement to existing clinical technology. During prolonged periods of wear, it is possible that impacts exceeding the yield stress of the polyurethane foam (≈0.3 MPa, see Figure S4, Supporting Information) will cause collapse of the foam cell structure and concomitant damage of the cast. Further experiments with human subjects would be required to assess the stability of the cast over extended periods of wear (i.e., weeks) and under stresses that the casts are subjected to during daily activities or accidental impacts.

4. Conclusion

The casting strategy proposed in this work is designed to save time and effort while minimizing complications associated with

**ADVANCED
SCIENCE NEWS**

www.advancedsciencenews.com

**ADVANCED
MATERIALS
TECHNOLOGIES**

www.advmattechnol.de

Table 1. Compilation of data from three-point flexural tests. Uncertainties are reported as 95% confidence intervals obtained from three independent experiments for each material.

Material	Stiffness [N mm^{-1}][a]	Strength** [J][b]	Mass [g]	Strength-weight ratio [J kg^{-1}]
Dense foam FFC	66 ± 10	3.3 ± 0.16	222 ± 7	14.9
Fiberglass	45 ± 14	2.4 ± 0.45	168 ± 8	14.3
Light foam FFC	20 ± 9	0.9 ± 0.63	156 ± 8	5.8
Plaster	14 ± 7	0.8 ± 0.22	161 ± 2	5.0
Soft fiberglass	2 ± 1	0.1 ± 0.04	160 ± 6	0.6

[a]Calculated from the slope of the force versus displacement up to a displacement of 0.5 cm; [b]Calculated as the numerical integral of the force to a displacement of 1 cm.

both cast application and removal. This strategy also provides a comfortable, lightweight, water-resistant, and impact-resistant solution. Given that i) the cast is amenable to high throughput manufacturing, ii) the materials required are inexpensive (≈$10 USD per cast; Table S1, Supporting Information), and iii) an orthopedic cast is classified by the Food and Drug Administration of the United States as a Class I medical device, subject to less strict regulations, the proposed technology could be rapidly translated to clinical use for situations in which limited orthopedic casting expertise is available (e.g., urgent care facilities, developing countries), or if temporary stabilization is required while awaiting an appointment with an orthopedic specialist.

A wide variety of casting strategies exist for clinicians to use in their treatment plans, encompassing a range of stability provided for the patient, depending on their unique fracture and lifestyle. These options can be categorized based on the level of stability they provide, ranging from internal fixation[37] for severe, comminuted fractures (i.e., when the bone breaks into three or more pieces), to plaster of Paris and fiberglass casts for displaced fractures, and custom thermoplastic or off-the-shelf splints for nondisplaced fracture and sprains. We envision that the FFC would fall between fiberglass and custom thermoformable casts on this "ladder" of stability due to its circumferential coverage, conformable contact, and mechanical stiffness.

For the FFC to be used in a clinical setting, further optimization of the foam activation and injection process is desirable. While the mixing and injection process we used in testing employs a syringe, which is commonly used by healthcare professionals for the administration of various treatments, our strategy is also amenable to a more user-friendly approach that employs squeezable pouches of foam components that can be manually mixed. Such technology already exists commercially for soft foam packaging devices.[38] Future iterations of the FFC prototype could include replacement of the cuttable fabric band with a fastening mechanism for adjusting the pressure, adaptation of the casting strategy to different parts of the body (e.g., a kit for the stabilization of ankle injuries in the field), and incorporation of more environmentally friendly materials (e.g., recyclable or biodegradable).

The FFC has been tested only on participants without fractures. These trials were conducted to demonstrate the safety of the application and removal of the FFC relative to fiberglass and plaster casts, as the first step toward clinical testing. Clinical testing with patients that have sustained fractures will be necessary to evaluate the ability of the FFC to stabilize fractured limbs while ensuring safety of use over extended periods of time. Despite these remaining hurdles, the expanding

foam-fabric orthopedic casting strategy is a promising approach to form custom-fitting structures for a variety of wearable orthopedic, prosthetic, and protective devices.

5. Experimental Section

Materials: A nylon knit-thermoplastic polyurethane (TPU) laminate (TS-100B, Eastex Products) was used for the fabric of the outer sleeve of the cast. A knit spacer fabric (90% Polyester/10% Spandex, Fabric Wholesale Direct) was used for the inner sleeve of the cast. The increased softness and extensibility of inner knit spacer fabric relative to the outer laminate allowed to fabricate a cast with an inner sleeve that was smaller than the outer sleeve; the inner fabric was sewn into the cast in a prestrained state to prevent the formation of wrinkles during the foam expansion process. A thermoplastic elastomer, Stretchlon 200 vacuum bagging film, was used for the interior pouch. This material was heat-sealed for 50 s at a temperature of 150 °C and a pressure of 10 kPa. The thermoplastic pouch and channels were patterned using unbleached SMARTAKE parchment paper baking sheets (9×13″). For all experiments involving the replica forearm and human subjects, Smooth-On FOAM-iT! 3 was employed as the expanding foam. Equal volumes of parts A and B were poured into the 100 mL syringe and then shaken vigorously for about 45 s before injection into the cast. For the three-point bending experiments, a denser foam (Smooth-On FOAM-iT! 5) was also employed for comparison.

Sewing: All sewing steps were completed with a Bernina 435 sewing machine with a walking foot attachment. A standard lockstitch was employed for all seams. For certain steps, such as sewing around the thumbhole of the cast, the pressure of the walking foot was reduced to facilitate the alignment of stacked materials and prevent wrinkling in the fabrics.

Laser Cutting: Patterning of materials was performed with a 60 W CO$_2$ laser (VLS 6.60, Universal Laser Systems) using the vector cutting mode and a 2.0 lens positioned at a focal length of 50 mm. A laser power of 30% and a speed of 50% were employed for the cutting of all materials.

X-Ray Computed Tomography (CT): CT images were acquired with a Nikon X-tek HMXST225 imaging system at the Center for Nanoscale Systems at Harvard University. X-rays were produced from an X-ray tube containing a tungsten target, operating at a voltage of 85 kV and a current of 115 μA. A total acquisition time of ≈110 min was employed, with two frames acquired per projection. To enhance the X-ray absorption of the inner lining, the fabric was soaked in an aqueous solution containing 3.05% potassium iodide and 1.85% iodine (Innovating Science), and then allowed to dry within a fume hood before being incorporated into the cast.

Scanning Electron Microscopy (SEM): SEM images were acquired using a Zeiss FESEM Ultra Plus microscope, at an operating voltage of 10 kV and a magnification of 74x. All samples were coated with a thin film of platinum (using a sputtering process) prior to imaging to prevent excess build-up of charge on the surface of the sample.

Mechanical Testing: Mechanical tests were performed using an Instron testing system series 5560 with dual column tabletop model 5566 and

**ADVANCED
SCIENCE NEWS**

www.advancedsciencenews.com

**ADVANCED
MATERIALS
TECHNOLOGIES**

www.advmattechnol.de

a 10 kN load cell. All experiments were performed at a loading rate of 50 mm min⁻¹.

Flexural Testing: Plaster, fiberglass, and soft casts were formed by wrapping casting tape around a polyvinyl chloride pipe with a length of 31 cm and an outer diameter of 10 cm. Casts were wrapped in accordance with orthopedic and manufacturer recommendations by overlapping the tape by approximately one half the width of the tape. All casts were left to fully cure for 5 days prior to testing. The resulting casts were four layers thick, with an inner diameter of 10 cm and an outer diameter of ≈11 cm. Foam fabric casts were made to be the same length as fiberglass and plaster casts (31 cm). During flexural testing, the hollow, cylindrical samples were stabilized using two 3D-printed support stands. A loading rate of 50 mm min−1 was applied until failure (defined by substantial buckling of the structure).

Capacitive Pressure Sensor: Capacitive pressure sensors were fabricated following the method outlined by Atalay et al. and Sanchez et al.[34,35] Each sensor was consisted of two layers of a conductive knit textile (Shieldex Technik-tex P130+B, V Technical Textiles Inc.) separated by a spacer knit fabric (90% Polyester/10% Spandex, Fabric Wholesale Direct), which acts as a dielectric layer. The three textile layers were laminated together using a thermoplastic film (3405, HeatnBond ultrahold iron-on adhesive) and heat-sealed at a temperature of 110 °C for a duration of 30 s. The conductive textile layers included excess fabric that was cut into opposing channels to allow for a soldered connection to the electrical leads of a capacitance meter. Capacitance was recorded with a B&K Precision 878B Dual Display Handheld Universal LCR Meter, operating at a frequency of 10 kHz. The sensor was connected by USB to a computer, and the serial data were recorded and analyzed using Python.

Human Subject Testing: This study was reviewed and approved by Harvard's Committee on the Use of Human Subjects (CUHS), which serves as the University-area Institutional Review Board (IRB). All methods were carried out in accordance with the approved study protocol. A total of seven healthy adult subjects in the range of 20–40 years of age participated in this study (four male and three female participants). All participants provided written informed consent before their participation, after the nature and the possible consequences of the studies were explained.

Statistical Analysis: Values of pressure recorded by the capacitive pressure sensor were obtained using the following procedure. Prior to each experiment, the sensor was calibrated using a medical grade pressure cuff placed over both the cast and the sensor. The pressure was manually increased in increments of 10 mmHg and held for 10 s at each pressure while the capacitance was recorded to construct a calibration curve using a linear regression. After removing the pressure cuff, the baseline was zeroed by subtracting out the initial capacitance (prior to injection of the foam). During the foam injection and expansion process, the capacitance values were divided by the slope of the linear calibration curve to obtain the pressure. For the three-point flexural experiments, mean values and 95% confidence intervals for the stiffness, strength, and mass of the hollow cylindrical specimens were obtained by repeating the experiments three times for each material and using the corresponding value from the *t*-distribution to convert the standard deviation to 95% confidence intervals. All data processing and statistical analysis was performed using the Python programming language and Microsoft Excel software.

Supporting Information

Supporting Information is available from the Wiley Online Library or from the author.

Conflict of Interest

G.M.W. acknowledges an equity interest and board position in Soft Robotics, Inc. A patent application has been submitted for this technology (PCT/US20/58566).

Data Availability Statement

The data that support the findings of this study are available from the corresponding author upon reasonable request.

[1] J. A. Buza, T. Einhorn, *Clin. Cases Miner. Bone Metab.* **2016**, *13*, 101.

[2] K. Kowalski, D. Pitcher, B. Bickley, *Mil. Med.* **2002**, *1678*, 657.

[3] S. Nguyen, M. McDowell, J. Schlechter, *World J. Orthop.* **2016**, *7*, 539.

[4] B. J. Shore, S. Hutchinson, M. Harris, D. S. Bae, L. A. Kalish, W. Maxwell, P. Waters, *J. Bone Jt. Surg., Am. Vol.* **2014**, *96*, e31.

[5] V. Sanchez, C. J. Walsh, R. J. Wood, *Adv. Funct. Mater.* **2021**, *31*, 2008278.

[6] K. Kleis, J. A. Schlechter, J. D. Doan, C. L. Farnsworth, E. W. Edmonds, *J. Pediatr. Orthop.* **2019**, *39*, 302.

[7] D. S. Bae, H. Lynch, K. Jamieson, C. W. Yu-Moe, C. Roussin, *J. Bone Jt. Surg., Am. Vol.* **2017**, *99*, e94.

[8] M. Halanski, K. J. Noonan, *J. Am. Acad. Orthop. Surg.* **2008**, *16*, 30.

[9] F. D. Shuler, F. N. Grisafi, *J. Bone Jt. Surg., Am. Vol.* **2008**, *90*, 2626.

[10] N. Patel, L. Wilson, G. Wansbrough, *Injury* **2016**, *47*, 2258.

[11] A. S. Boyd, H. J. Benjamin, C. Asplund, *Am. Fam. Physician* **2009**, *79*, 16.

[12] B. G. Santoni, J. R. Aira, M. A. Diaz, T. Kyle Stoops, P. Simon, *Clin. Biomech.* **2017**, *47*, 20.

[13] F. Buonamici, R. Furferi, L. Governi, S. Lazzeri, K. S. McGreevy, M. Servi, E. Talanti, F. Uccheddu, Y. Volpe, *Visual Comput.* **2020**, *36*, 375.

[14] F. Blaya, P. S. Pedro, J. L. Silva, R. D'Amato, E. S. Heras, J. A. Juanes, *J. Med. Syst.* **2018**, *42*, 54.

[15] F. Buonamici, R. Furferi, L. Governi, S. Lazzeri, K. S. McGreevy, M. Servi, E. Talanti, F. Uccheddu, Y. Volpe, *Comput.-Aided Des. Appl.* **2018**, *16*, 25.

[16] J. Troutner, A. S. Moy, A. Stevenson, A. Seshadri, E. Wisniewski, B. Lung, K. Furbee, V. A. Hogg-Cornejo, US20180153745A1, **2018**.

[17] R. R. Rao, L. A. Mondy, K. N. Long, M. C. Celina, N. Wyatt, C. C. Roberts, M. M. Soehnel, V. E. Brunini, *AIChE J.* **2017**, *63*, 2945.

[18] S. J. Yeo, M. J. Oh, P. J. Yoo, *Adv. Mater.* **2018**, *31*, 1803670.

[19] P. S. D. Patel, D. E. T. Shepherd, D. W. L. Hukins, *BMC Musculoskeletal Disord.* **2008**, *9*, 137.

[20] K. D. Martin, US9427489B2, **2016**.

[21] A. Goosens, T. Detienne, M. Bruz, *Contact Dermatitis* **2002**, *47*, 304.

[22] M. Thirumal, D. Khastgir, N. K. Singha, B. S. Manjunath, Y. P. Naik, *J. Appl. Polym. Sci.* **2008**, *108*, 1810.

[23] K. W. Nellans, E. Kowalski, K. C. Chung, *Hand Clin.* **2012**, *28*, 113.

[24] L. M. Ryan, S. J. Teach, K. Searcy, S. A. Singer, R. Wood, J. L. Wright, J. M. Chamberlain, *J. Trauma: Inj., Infect., Crit. Care* **2010**, *69*, S200.

[25] M. J. Shauver, H. Yin, M. Banerjee, K. C. Chung, *J. Hand Surg. Am.* **2011**, *36*, 1282.

[26] J. A. Garcia-Rodriguez, P. D. Longino, I. Johnston, *Can. Fam. Physician* **2018**, *64*, 746.

[27] L. M. Adkins, *Pediatr. Nurs.* **1997**, *23*, 422.

[28] A. T. Berman, B. G. Parks, *J. Orthop. Trauma* **1990**, *4*, 85.

[29] F. Freislederer, T. Berberich, T. O. Erb, J. Mayr, *Children* **2020**, *7*, 229.

[30] J. P. Smiles, M. Simonian, M. Zhang, S. Digby, S. Vidler, S. Flannagan, *EMA – Emerg. Med. Australas.* **2020**, *32*, 1015.

[31] M. Ahmadi, R. Rajamani, S. Sezen, *IEEE Sens. Lett.* **2017**, *1*, 2500604.

[32] S. Chaudhury, A. Hazlerigg, A. Vusirikala, J. Nguyen, S. Matthews, *World J. Orthop.* **2017**, *8*, 170.

[33] L. R. Mohler, R. A. Pedowitz, T. P. Byrne, D. H. Gershuni, *Clin. Orthop. Relat. Res.* **1996**, *322*, 262.

[34] O. Atalay, A. Atalay, J. Gafford, C. Walsh, *Adv. Mater. Technol.* **2018**, *3*, 1700237.

[35] V. Sanchez, C. J. Payne, D. J. Preston, J. T. Alvarez, J. C. Weaver, A. T. Atalay, M. Boyvat, D. M. Vogt, R. J. Wood, G. M. Whitesides, C. J. Walsh, *Adv. Mater. Technol.* **2020**, *5*, 2000383.

[36] W. M. Mihalko, A. J. Beaudoin, W. R. Krause, *J. Orthop. Trauma* **1989**, *3*, 57.

[37] S. Boydstun, L. Nash, G. M. Rayan, *J. Hand Surg. Asian-Pac. Vol.* **2019**, *24*, 412.

[38] J. Yang, X. Zhao, Q. Li, Z. Ji, *Emerging Mater. Res.* **2017**, *6*, 60.